Eur. Phys. J. D **33**, 221–228 (2005)
DOI: 10.1140/epjd/e2005-00038-4

THE EUROPEAN PHYSICAL JOURNAL D

The dominant "heating" mode: bending excitation of water molecules by low-energy positron impact

T. Nishimura and F.A. Gianturco[a]

Department of Chemistry and INFM, The University of Rome "La Sapienza", Piazzale A. Moro 5, 00185 Roma, Italy

Received 13 December 2004 / Received in final form 17 February 2005
Published online 12 April 2005 –

Abstract. We report a quantum dynamical treatment of the vibrational excitation of the bending mode of water molecules by collision with low energy positrons in the energy regions close to threshold openings. The exact vibrationally coupled-channel equations derived for the total $e^+ - H_2O$ system are solved in a Body-Fixed-Vibrational-Coupled-Channels (BF-VCC) reference frame, using a single-center expansion of the total wavefunction and of the interaction potential. The vibrationally inelastic cross-sections for transitions from the ground to the lowest excited state of the bending mode clearly show the bending excitation channel to be the dominant inelastic process at low collision energies. Comparisons with our earlier calculations for the other modes and for the excited processes induced by electron impact are also presented and analysed.

PACS. 34.85.+x Positron scattering – 34.90.+q Other topics in atomic and molecular collision processes and interactions (restricted to new topics in section 34) – 34.80.-i Electron scattering

1 Introduction

Collision systems involving the water (H_2O) molecule as a partner are of significant, practical interest in a variety of fields like plasma processing, radiation physics, atmospheric physics, and biological matter (see e.g. [1,2]). In particular, the vibrational excitation of the normal modes is an important mechanism because excited molecules are prominent in other, ensuing reactive processes [3,4]. When dealing with low incident energies of the leptonic projectiles like electrons (e^-) and positrons (e^+), most of the energy transfer occurs, as we shall see, at collision energies of less than a few tens of electron volts, thereby making such processes even more relevant at the chemical level. As a result of the fundamental interest held by the role of vibrations in so many research domains there has been quite a number of measurements ([5–8] and references therein) and calculations (e.g. [9–11] and references quoted there) which have dealt with the features of vibrationally inelastic cross-sections for electrons on H_2O. In the case of positrons, on the other hand, no excitation cross-sections for H_2O target have been reported so far, both theoretically and experimentally, apart from a brief discussion of its stretching modes behaviour recently carried out by us [12].

The H_2O molecule is a polar target that belongs to the C_{2v} point group and possesses three different vibrational modes: the symmetric stretching (ν_1), the bending (ν_2) and the antisymmetric stretching (ν_3). Since all modes are infrared (IR) active, and therefore an additional long-range interaction due to the induced dipole moment is playing an important role in the processes, we shall further analyse this feature more in detail (see Tab. 1). Furthermore, due to remarkable developments in experimental techniques, very recently measured electron energy loss spectra obtained with 10 meV of FWHM have revealed that the ν_3 mode is excited much less than the ν_1 at low energies (between 0.05–3 eV above the thresholds [8]). In the case of the positrons, however, the higher resolution required is not yet available since the current best resolution of measurements is around 18 meV of FWHM [13]. As a matter of fact, even in the case of electron scattering, the excitations of the ν_1 and ν_3 modes have not been resolved, except for the very limited data recently measured by Allan and Moreira [8].

These situations have thus stimulated the interest of theoreticians and have spurred computations to provide predictions and explanations on how the phenomenon is occurring at the nanoscopic level. The vibrational excitation processes are here considered as taking place among the lowest energy levels of all the H_2O modes, and therefore they could be treated as occurring separately within each of the vibrations with different fundamental frequencies and symmetries. This is clearly an important simplification that is usually justified in cases where resonant effects play a negligible role and therefore for situations where the direct excitation mechanisms could be thought of as acting in a decoupled fashion among the different

[a] e-mail: fa.gianturco@caspur.it

Table 1. Vibrational modes of H_2O molecule.

Mode	Frequency (eV)		Irreducible	Activity
	exp. [a]	cal.	representation	
ν_1 (symm. stretch)	0.4535	0.4842	A_1	Infrared
ν_2 (bending)	0.1978	0.2235	A_1	Infrared
ν_3 (antisymm. stretch)	0.4657	0.4948	B_2	Infrared

[a] The recommended values based on experiments [28].

modes. Since positron projectiles are often considered not to give rise to resonant processes in molecular environments [9], we decided to keep this decoupling approximation in our present study. We shall try to understand how the separate vibrational excitation cross-sections depend on the feature of the specific mode and on the charge of projectile, without considering for the moment the further complication coming from the mixing of modes. The present work extends our earlier results on this system [12] in the sense that (i) it completes the normal mode analysis by adding new results for the bending excitation, and (ii) tries to compare in some detail the behaviour of the positron-impact excitation cross-section with that, already analysed by earlier experiments and calculations, of electron impact excitation processes.

Since the experimental studies on electron-impact excitation [8] indicate the $(v = 0 \rightarrow v' = 1)$ transition to be the dominant process and that the gas molecular targets are taken to be, in the main, in their ground vibrational states, we shall limit our present analysis to that computed transition, although there is no computational limitation in considering further excited states (either final or initial) for the title molecule.

The following section outlines our theoretical approach while Section 3 presents and discusses our results in relation with previous theoretical data obtained for electron-impact excitation [14]. Our conclusions are summarized in Section 4. Atomic units (au) are used throughout unless otherwise stated.

2 The theoretical method

2.1 General outline

Since the details of the present theory have already been reported by us [15,16], we provide here only a brief reminder of them. To obtain vibrational excitation cross-sections we need to solve the Schrödinger equation of the total system for the wavefunction Ψ, at a fixed value of the total energy E. The total Hamiltonian is represented by the sum of operators that include the molecular Hamiltonian, the kinetic energy for the scattered projectile and the interaction between the incident projectile and the target molecule. The molecular Hamiltonian only consists of the rotational and vibrational parts, i.e. before and after the collision the molecular electronic wavefunction is always that of the ground state.

We further assume that the molecular orientation remains fixed during the collision time, since the molecular rotation is usually slower when compared with the velocity of the projectile at the energies we are considering. This is called the fixed nuclear orientation (FNO) approximation [17], and corresponds to ignoring the rotational Hamiltonian. Then, the total wavefunction could be expanded as

$$\Psi(\mathbf{r} \mid \mathbf{R}) = r^{-1} \sum_{l\nu n} u_{l\nu n}\ (r)\ X_{l\nu}(\widehat{\mathbf{r}})\ \chi_n(\mathbf{R}). \qquad (1)$$

Here χ_n is the vibrational wavefunction of the molecule, with the vibrational quantum numbers of the normal modes represented by the index n, with $n \equiv (n_1, n_2, n_3)$ for H_2O. The variables $\mathbf{R}$ and $\mathbf{r}$ denote the molecular nuclear geometry and the position vector of the scattered projectile from the center-of-mass of the target. The unknown radial functions $u_{l\nu n}$ describe the coefficients of the scattered wavefunction of the projectile, and the $X_{l\nu}$ are the symmetry-adapted angular basis functions [16]. The symbol ν in equation (1) globally stands for the indices specifying the irreducible representation and for those distinguishing its degenerate members. The symmetry of the target initial state is labelled as $|l_0\nu_0\rangle$.

After substituting equation (1) into the Schrödinger equation of the total system under the FNO approximation, we obtain a set of full coupled-channel equations for each $u_{l\nu n}\ (r)$ function that now explicitly includes the vibrational channels. These are called the body-fixed vibrational close-coupling (BF-VCC) equations (see e.g. [15])

$$\left\{\frac{d^2}{dr^2} - \frac{l(l+1)}{r^2} + k_n^2\right\} u_{l\nu n}(r) = 2 \sum_{l'\nu'n'} \langle l\nu n|V|l'\nu'n'\rangle\ u_{l'\nu'n'}(r), \qquad (2)$$

where $k_n^2 = 2\ (E - E_n^{vib.})$ with $E_n^{vib.}$ being the energy of the specific molecular state $|n\rangle$. We should further stress that, given the low-level of vibrational excitation caused by positron impact at the considered energies, the contributions from intermode couplings have been disregarded. Any of the elements of the interaction matrix in equation (2) is given by

$$\langle l\nu n|V|l'\nu'n'\rangle = \sum_{l_0\nu_0} \langle n|V_{l_0\nu_0}|n'\rangle \times \int d\widehat{\mathbf{r}}\ X_{l\nu}(\widehat{\mathbf{r}})^*\ X_{l_0\nu_0}(\widehat{\mathbf{r}})\ X_{l'\nu'}(\widehat{\mathbf{r}}). \qquad (3)$$

Furthermore, in the present calculations we have also disregarded the effects from both real and virtual Ps formation during the scattering event. While the neglect of intermode coupling may not be of major significance when dealing with positron scattering at low energies where (contrary to the electron case [18]) resonances are usually negligible, it is hard to assess the effects of neglecting the additional "reactive" channel of Ps formation. The only qualitative justification could be had by considering the low collision energies we shall be examining (below Ps formation) and by surmising that virtual excitations are somewhat already "folded" within our modelling of correlation-polarization forces [20]. Thus, we compute matrix elements of the following type

$$\langle n|V_{l_0\nu_0}|n'\rangle = \int d\mathbf{R}\ \{\chi_n(\mathbf{R})\}^* V_{l_0\nu_0}(r \mid \mathbf{R})\{\chi_{n'}(\mathbf{R})\} \quad (4)$$

for the ground state of the initial target, $|l_0\nu_0\rangle$. This method is essentially a generalization of the method proposed long ago (called the "hybrid theory") for the much simpler case of a diatomic molecule [19]. When solving equation (2) under the usual boundary conditions, we obtain the K-matrix elements and the corresponding T-matrix. Therefore, the integral cross-section for the vibrationally inelastic scattering is given by

$$Q(n \to n') = \frac{\pi}{k_n^2} \sum_{l\nu} \sum_{l'\nu'} |T^{l\nu n}_{l'\nu' n'}|^2 \quad (5)$$

where $T^{l\nu n}_{l'\nu' n'}$ is one of the T-matrix elements (see Ref. [17] for further details on the specific factors involved).

The interaction between the impinging projectile and the molecular target is represented in the form of a local potential. In the case of positron the interaction consists of a sum of the V^{st} and a positron correlation-polarization (V^{pcp}) terms. To obtain the correlation-polarization terms in the short range of the interaction region, we make use of simple, parameter-free model potentials based on a positron-electron correlation terms suggested by Boronski and Nieminen [20] and connected to long-range polarizability contributions similarly to what was done for electron as projectiles [21]. We have given many times before our own implementation of the above model (e.g. see [15,16]) and therefore we will not be dwelling on it here. Briefly, the V^{pcp} term is given using the correlation energy ε^{corr} in the framework of a homogeneous electron gas [22],

$$V^{pcp}(\mathbf{r} \mid \mathbf{R}) = \frac{d}{d\rho}\ \left\{\rho\ (\mathbf{r} \mid \mathbf{R})\ \varepsilon^{e-e}[\rho\ (\mathbf{r} \mid \mathbf{R})]\right\}, \quad (6)$$

where ρ denotes the undistorted electron density of the target. In our present formulation of this model, the short-range V^{pcp} is connected smoothly to the asymptotic form (V^{pol}) of its spherical component,when they cross at distances of about $4.5a_o$ from the molecular center-of-mass

$$V^{pol}(\mathbf{r} \mid \mathbf{R}) \sim_{\mathrm{r}\to\infty} -\frac{\alpha_0(\mathbf{R})}{2\mathbf{r}^4}. \quad (7)$$

Here, α_0 is the spherical dipole component of the target polarizability.

We have already noted that an incident positron has the additional possibility of taking up one of the bound electrons of the target molecule to form a positronium (Ps) atom, when the collision energy is above the threshold for the Ps formation energy (5.8 eV for H_2O). Throughout the present study, however, no Ps formation channel has been taken into account and the collision energies have been considered as being below that threshold value.

It should also be noted that the above model of correlation-polarisation forces in the case of positron-molecule interaction is somewhat similar to the one we have implemented to describe electron-H_2O interaction [14]. In that work we showed that the ensuing quantum dynamics (the same employed in the present study) provided a very realistic description of the vibrationally inelastic scattering for $e^- - H_2O$ collisions. We thus expect that the present treatment for positron scattering might also predict rather realistically the corresponding vibrationally inelastic processes.

2.2 Numerical details

The target wavefunction of the electronic ground state for H_2O was calculated at the self-consistent field (SCF) level by solving the Hartree-Fock (HF) equations for a single-determinant representation of the target electrons. We use our familiar single-center expansion method [23] applied to a multicenter Gaussian-type orbital (GTO) expansion, and the basis set employed was obtained via the *Gaussian 98* package [24]. The GTO basis sets we have chosen are those of D95* type which consist of $(9s5p1d)/[4s2p1d]$ for oxygen and $(4s)/[2s]$ for hydrogen which is the same as that employed in our very recent calculations+ [12]. The H_2O molecule is placed in xz-plane and the z-axis is taken along the C_2 symmetry axis with the oxygen atom on the positive side.

The terms of the multipolar expansion of the interaction potential in equation (3) were retained up to $l_{0,max}$, and the scattered wavefunction of the electron in equation (1) was expanded, with the inclusion of the lowest two vibrational states (000) and (100), (010) or (001), up to l_{max} which yields inelastic cross-section values converged within about 5%. For specific information on all the required parameters and properties for each of the vibrational modes of the present work, see Table 2 and also our earlier studies [12,14].

In order to solve the coupled-channel equations by means of standard Green's function techniques, equation (2) is rewritten as an integral equation (a Volterra equation: for details, see [25,26]). Selected test of the vibrational close-coupling convergence were carried out at specific energies: we found in both cases that the inclusion of a third vibrational state (i.e. $n = 2$) did not modify significantly the values of the relevant K-matrix elements.

In the interaction potential of equation (4) we include initial and final vibrational wavefunctions with respect to the variable $\mathbf{R}$, the molecular bond lengths for the

Table 2. Computational details of the two-state BF-VCC calculation.

Normal mode	Point group	e^- / e^+ $l_{0,max}$	scattering l_{max}	Maximum number of coupled channels
ν_1	C_{2v}	20	10	$A_1 = 72,\ A_2 = 50,\ B_1 = 60,\ B_2 = 60$
ν_2	C_{2v}	20	10	$A_1 = 72,\ A_2 = 50,\ B_1 = 60,\ B_2 = 60$
ν_3	C_s	20	10	$A = 132,\ B = 110$

two stretching modes of ν_1 and ν_3 and to the molecular angle for the ν_2 bending mode. They were made to vary in ranges supporting vibrational energy levels up to and above $n = 4$. For the asymptotic part of V^{pcp}, i.e. V^{pol}, we first computed the spherical polarisability, α_0, from the target wavefunction with the GTO basis set D95*, and then scaled our results to the experimental value (9.92 au) taken to be valid for the molecular equilibrium geometry [27]. Such ad hoc renormalization has the advantage of accounting in a more realistic way for the behaviour of polarisation forces in the long range regions, and also to compensate for the limitation of our basis set expansion in its use of more diffuse functions which would provide better virtual orbitals for polarisability evaluation. Figure 1 reports pictorially the behaviour of the scaled and unscaled polarizability values over the range of normal mode deformations examined here. Due to smaller contributions from the nonspherical parts of the dipole polarisability [27] we decided not to include them in the present calculations.

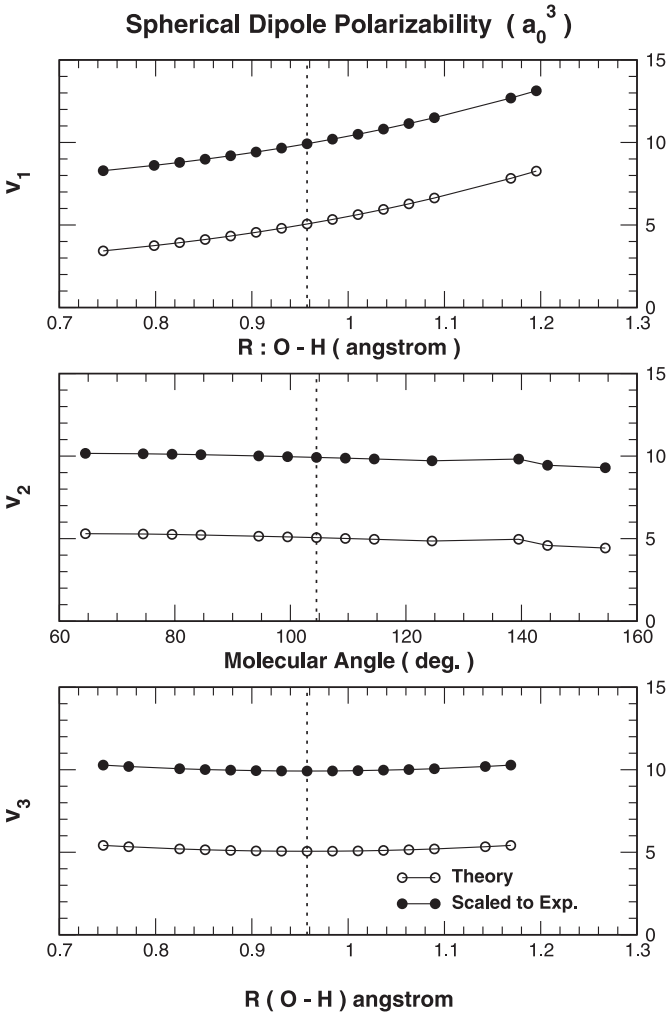

Fig. 1. Computed dependence of the spherical dipole polarisability on the changes of each of the three normal coordinate. The experimental value at the equilibrium geometry is taken from reference [9].

3 Results and discussion

The pseudo one-dimensional potential energy curves associated to each of the normal coordinates of H_2O allowed us to evaluate, in a preparatory stage, the range of bond length and bond angle values needed to support the first five vibrational bound states for the three normal modes of the title molecule. We have already reported [12] the contributions to the full interaction from the permanent dipole moment of water during the vibrations of the nuclei: our calculations show fair agreement with the experimental value that corresponds to equilibrium ($\nu_i = 0$) geometry in the gas phase [9], while nothing is known about direct dipole values for the "hot" molecular gas.

The approximation that a simple, mode-independent scaling is sufficient for correctly describing the α_0 (R_n) behavior (R_n) being any of the normal mode coordinates, (see also Table 3 for the relation between the R_n and the symmetry coordinates S_n) has been tested before [15] and turned out to yield good agreement with experiments. Our recent comparison with experiments [5–7] for electron-H_2O vibrational inelasticity also provided good agreement with them [14], thus suggesting that the present handling of long-range polarization effects gives a reasonable description of their behaviour during the scattering process.

The results we report in Figure 2 show the computed behavior of all three vibrationally inelastic partial cross-sections for H_2O by positron impact. We clearly see there that the $(0 \rightarrow 1)$ excitation cross-section via the bending mode exhibits by far the largest values and remains always the most efficient excitation pathway for water by positron impact, thus confirming our earlier findings [12] on the rather low efficiency of collisional heating of H_2O by positron via the stretching modes only. Furthermore, we also see in that figure how all three modes exhibit strong peaks at the openings of their respective thresholds, this feature being also stronger for the bending mode. We also found that to go beyond the two-state approximation for the vibrational states included in the BF-VCC equations did not have any noticeable effect

Table 3. The transformation from the symmetry coordinates S_n to the normal coordinates R_n is given as $S_j = \sum_k L_{jk} R_k$ with the L-matrix from John et al. [29]. r_i (r_{eq}): the bond length (equilibrium) of O−H$_i$ (Å), θ: the molecular angle (rad.).

Normal mode	Symmetry coordinates (Å)	L-matrix elements (amu$^{-1/2}$)
ν_1	$\Delta S_1 = 2^{-1/2}\ (\Delta r_1 + \Delta r_2)$	$L_{11} = \ 1.017841,\ L_{12} = -0.056171$
ν_2	$\Delta S_2 = r_{eq}\ \Delta\theta$	$L_{21} = -0.003374,\ L_{22} = \ 1.463114$
ν_3	$\Delta S_3 = 2^{-1/2}\ (\Delta r_1 - \Delta r_2)$	$L_{33} = 1.034581$

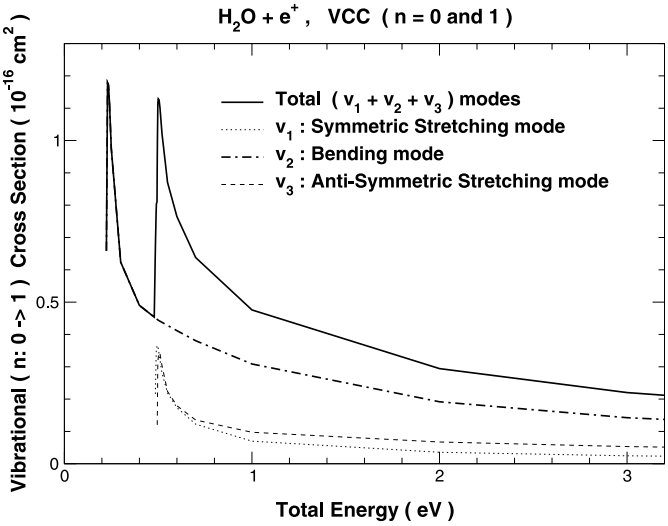

Fig. 2. Vibrational excitation cross-sections for positron scattering computed within the 2-state BF-VCC method from the ground state (000) to the lowest excited states of (100) (dotted curve), (010) (chain curve) and (001) (broken curve). The solid curve represents the sum of the cross-sections for the three modes.

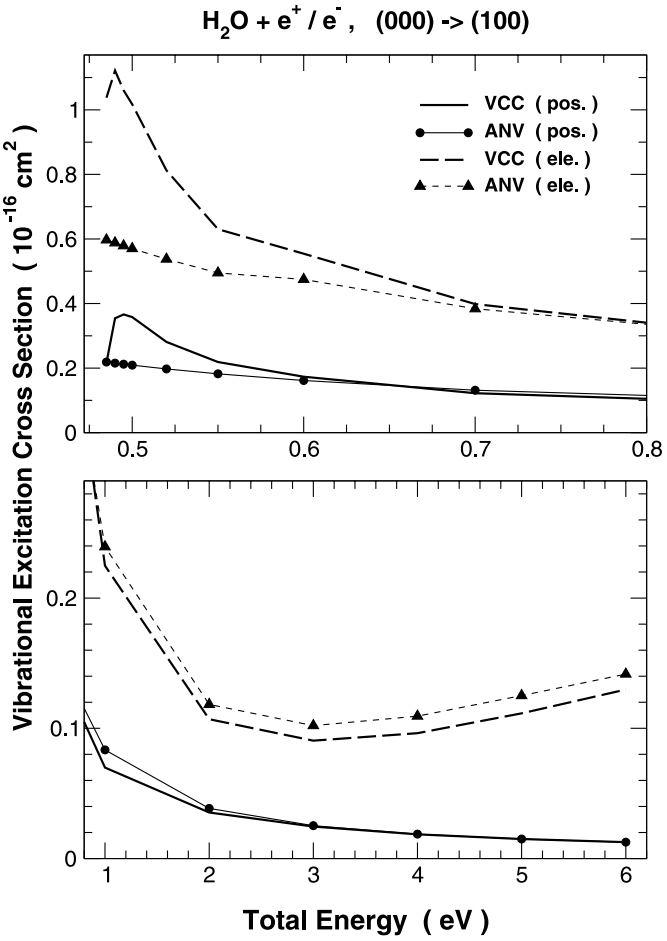

Fig. 3. Vibrational cross-sections for the (100) state computed within the 2-state BF-VCC and the ANV methods for both electron and positron projectiles in the low energy region (upper panel) and in the higher energy range (lower panel).

on the relevant K-matrix elements. This rapid convergence of the vibrational coupled-channel expansion indicates the rather weak deformation of the molecular vibrational modes which is induced by the impinging positron projectiles, and appears to rule out the possible presence of close-channel resonances (i.e. Feshbach resonances), at least from initially "cold" molecular targets. The total inelastic cross-sections, summed over the three normal modes, are quite substantial at threshold but do not show any additional, significant feature when one moves away from the threshold peaks, contrary to what happens for the electron-impact excitation processes [14].

Another aspect of the present work is the possibility to compare vibrationally excitation of water molecule in the gas phase by impact with the two charged leptons, e^+ and e^-. Since no experimental data exist for the former projectile, and since we have already found that our calculations for e^- projectile turn out to be in good agreement with experiments [14], we think that the present analysis of the inelastic cross-sections, for positron impact could also be taken as a rather realistic prediction and therefore could be compared with possible future experiments.

The results given by Figures 3, 4 and 5 report a comparison between our computed vibrationally inelastic cross-sections for both electron and positron as projectiles using the full interaction in both cases. Furthermore, in each figure we compare one of the normal modes over two different collision energy regions: the upper panels report the low-energy behavior just above each excitation threshold and up to about 0.8 eV of energy, while the lower panels show the inelastic cross-sections at higher collision energies and up to about 6.0 eV. The following comments could be made:

1. in the energy regions well above threshold (see lower panels) the inelastic cross-sections for $e^- - H_2O$ are invariably larger than those of positron. In those regions, in fact, the electron cross-sections show the onset of a

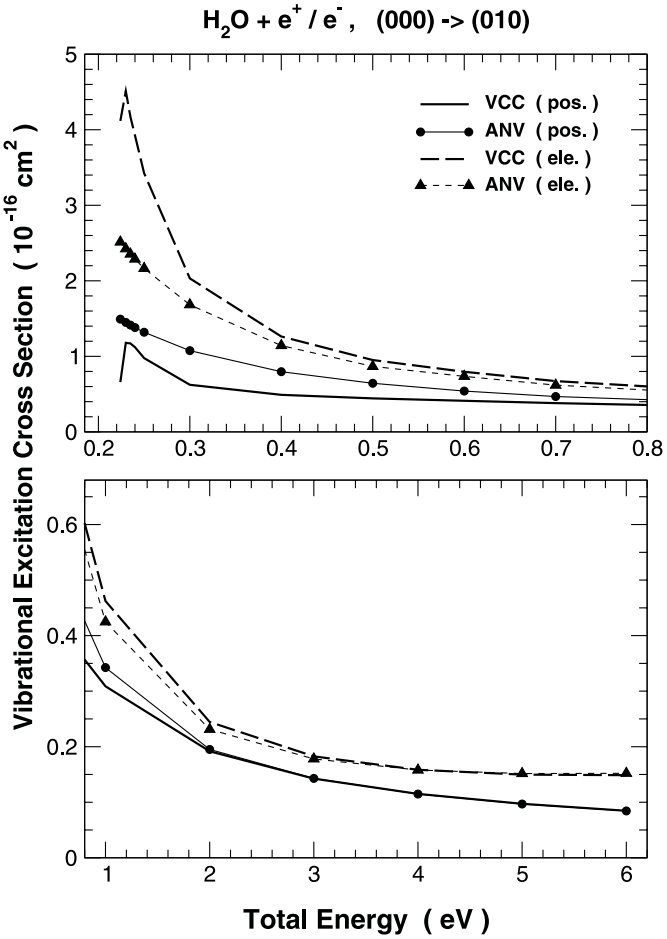

Fig. 4. Same as in Figure 3 but for the (010) state.

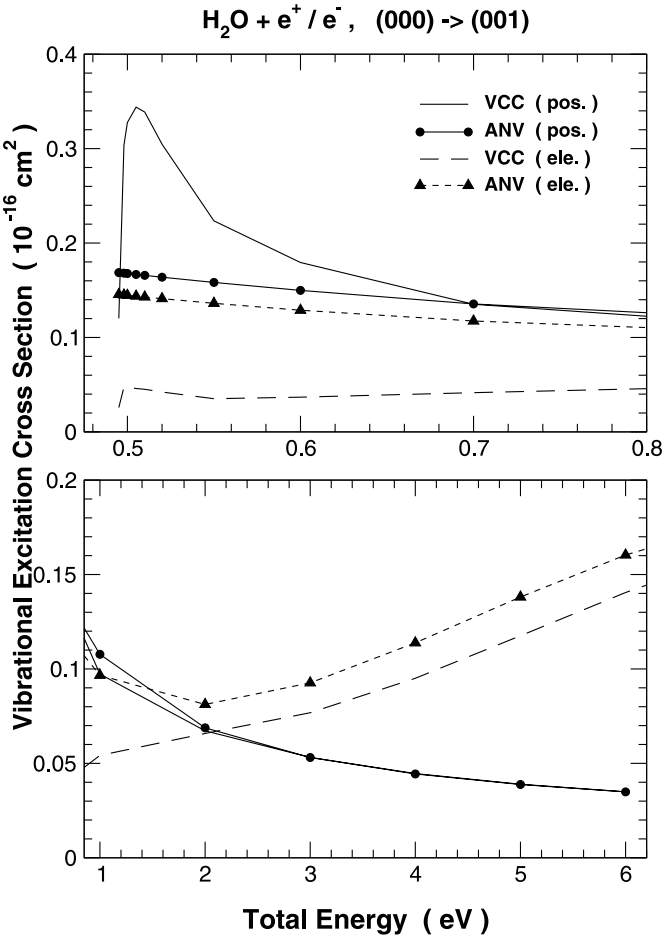

Fig. 5. Same as in Figure 3 but for the (001) state.

well-known broad resonance feature [8] which is indeed absent in e^+ scattering;

2. all BF-VCC calculations at the higher energies (given by the lower panels of those three figures) are well reproduced by the simpler calculations that use the adiabatic nuclear vibration (ANV) model [16] and therefore the latter could be just as profitably used to generate partial, integral inelastic cross-sections in that range of energy. This is a very interesting result in terms of the reliability of simpler dynamical models and has been already discussed in general terms for electron scattering (e.g. see the review of Ref. [17]);
3. on the other hand, marked differences between the ANV approximation and the correct, on-shell treatment of the vibrational dynamics appear as the collision energies decrease and get closer to the thresholds of the three modes: the ANV scheme clearly underestimates there the coupling dynamics of the inelastic processes (see upper panels of all three figures). The most marked departure from the adiabatic behavior is seen in Figure 5 for the case of the ν_3 mode, where near threshold the BF-VCC positron-induced cross-section is much larger than that for the case of the electron-induced excitation (dashed curve), while the corresponding ANV results for both projectiles are instead found to be very close to each other: in other words, the e^+ induced excitation of the ν_3 made excitation becomes larger than the corresponding ν_3 mode excitation by electron impact.

This feature could be qualitatively understood by considering that the positron projectile, at energies near the threshold opening, mostly samples the long-range polarizability region where the leading coefficient of the spherical dipole polarisability turns out to have a large derivative [12,14]. On the other hand, the electron motion at low energies is also strongly affected by the attractive nuclear contributions, which happen to describe for this mode the out of phase motion of the two H atoms, a feature that produces in the end cancellation effects in the total static interaction. As a consequence of it, the e^- impact excitation yields dynamically inelastic coupling matrix elements which are less efficient than in the case of e^+ impact for the case of the asymmetric stretching mode. This is an interesting result when one considers that, at least in the case of electron-impact excitation, the experimental detection of the single ν_3 mode is not possible but rather that the $(\nu_1 + \nu_3)$ excitation function is usually being detected in this system (e.g. see Ref. [8]). In the case of the electron-H_2O system, therefore, the strength of the signal appears to chiefly come from the

symmetric rather than the asymmetric mode excitation, at least this is what our computations suggest [14]). From the above considerations, and from the present calculations for positron-impact excitation, we thus see that the size of the ν_3 excitation by e^+ is indeed comparable with that of the ν_1 excitation by the same antiparticle and therefore their $(\nu_1 + \nu_3)$ sum could also become intense enough to be amenable to experimental detections: two weaker, but comparable, excitation cross-sections could then give rise to a measurable signal.

All the calculations reported by Figures 3, 4 and 5 further indicate rather clearly that the positron-induced molecular excitations are smaller than those caused by the electron, especially when collision energies move away from the thresholds, as illustrated by the results shown in the lower panels of those figures. Only for the bending excitation we see the electron data to remain still larger but closer in size to the e^+-impact cross-sections.

4 Summary and conclusions

In this work we have carried out calculations for the vibrationally inelastic cross-sections of the water molecule by low-energy impact with the leptonic particles, e^+ and further compared it with our previous results for e^- [14]. The theoretical treatment has been exact in terms of the dynamics of the inelastic process and the interaction forces have been described as sums of contributions obtained either exactly (the V^{st} contribution or via a parameter-free model treatment (the V^{pcp} contribution). The quality of the above interaction potential had been tested earlier for the case of the electron projectile by a comparison with existing experimental data [14], where agreement turned out to be good and gave us some confidence on the reliability of also using a similar modelling of the interaction forces when treating e^+ vibrational excitation processes.

The results of the inelastic cross-sections at energies well above the threshold openings (i.e. above about 1 eV) indicate that the e^- is invariably a more efficient "heater", in the sense that it transfers energy to the vibrational modes with greater probability than the e^+ projectile. Furthermore, the presence of a broad $(e^- - H_2O)$ resonance complex around 9 eV further provides an additional mechanism for vibrational inelasticity enhancement [14]. Such a mechanism is entirely absent in the case of the positron projectile that therefore shows lower efficiency in the excitational dynamics.

At collision energies near the vibrational thresholds, we found that inelastic cross-sections for both e^- and e^+ present a marked dipolar peak that strongly increases the cross-section values, although this effect is again stronger for electron than for positron impact. The only exception to this is the electron impact excitation of the ν_3 mode, where no peak is present at threshold for electron scattering while the positron-induced excitation exhibits a strong feature attributable to specific enhancement from the interplay between its long-range interaction and its static interaction caused by the out-of-phase vibrating H nuclei. In the case of e^- collisions, on the other hand, such motions lead to term cancellations (see before) due to the chiefly attractive static potentials for electrons.

The present calculations therefore indicate that positron-induced vibrational excitation processes in gaseous water molecule should be strong enough to be amenable to detection, especially at energies close to their thresholds. Furthermore, their values at higher energies should also be detectable in the case of the unresolved $(\nu_1 + \nu_3)$ energy losses, since their sum is seen from our calculations to remain not negligible due to the dominant contribution of the ν_3 mode. Our tentative explanation for such an effect is related to the dominance of long-range forces when slow positrons are interacting with polyatomic targets and are kept out of the molecular electronic charges by the dominantly repulsive static contributions. On the other hand, in the case of the electron-induced excitation, the nuclear motions of the two H atoms are out of phase in the ν_3 mode and the attractive Coulomb contributions undergo cancellations within the dominant partial waves that couple nuclear motions with the continuum electron during the inelastic dynamics. Therefore, since the e^+ projectile remains largely outside the nuclear region during the scattering, it causes the long-range contributions to its interaction with H_2O to remain dominant, thereby inducing a more marked inelasticity of the ν_3 mode during the collision. Our present calculations therefore are able to suggest that the $(\nu_1 + \nu_3)$ energy loss peak from positron experiments should be large enough to be amenable to detection by low-energy experiments that use this particular leptonic projectile.

The financial support of the Research Committee of the University of Rome "La Sapienza" (URLS), of the Ministry for University and Research (MUIR) and of the CASPUR supercomputing center is gratefully acknowledged. This work was also part of the European network EPIC, of which URLS is one of the Research nodes. Finally, one of us (TN) thanks the CASPUR supercomputing center for the awarding of a Research Fellowship.

References

1. T.E. Cravens, A. Korosmezey, Planet Space Sci. **34**, 961 (1986)
2. M.A. Ishii, M. Kimura, M. Inokuti, Phys. Rev. A **42**, 6486 (1990)
3. N.J. Mason, W.M. Johnstone, P. Akther, *Electron Collisions with Molecules, Clusters, and Surfaces*, edited by H. Ehrhardt, L.A. Morgan (New York, Plenum, 1994), p. 47
4. I. Krajcar-Bronic, M. Kimura, J. Chem. Phys. **103**, 7104 (1995)
5. G. Seng, F. Linder, J. Phys. B: At. Mol. Phys. **9**, 2539 (1976)
6. T.W. Shyn, S.Y. Cho, T.E. Cravens, Phys. Rev. A **38**, 678 (1988)
7. A.A.A. El-Zein, M.J. Brunger, W.R. Newell, J. Phys. B: At. Mol. Opt. Phys. **33**, 5033 (2000)
8. M. Allan, O. Moreira, J. Phys. B: At. Mol. Opt. Phys. **35**, L37 (2002)

9. T. Nishimura, Y. Itikawa, J. Phys. B: At. Mol. Opt. Phys. **28**, 1995 (1995)
10. O. Moreira, D.G. Thompson, B.M. McLaughlin, J. Phys. B: At. Mol. Opt. Phys. **34**, 3737 (2001)
11. R. Curik, P. Carsky, J. Phys. B: At. Mol. Opt. Phys. **36**, 2165 (2003)
12. T. Nishimura, F.A. Gianturco, Nucl. Inst. Meth. Phys. Res. B **221**, 24 (2004)
13. J.P. Sullivan, S.J. Gilbert, C.M. Surko, Phys. Rev. Lett. **86**, 1494 (2001)
14. T. Nishimura, F.A. Gianturco, Europhys. Lett. **65**, 179 (2004)
15. T. Nishimura, F.A. Gianturco, Phys. Rev. A **65**, 062703 (2002)
16. T. Nishimura, F.A. Gianturco, J. Phys. B: At. Mol. Opt. Phys. **35**, 2873 (2002)
17. Y. Itikawa, Int. Rev. Phys. Chem. **16**, 155 (1997)
18. E.g. see: T.N. Rescigno, W.A. Isaacs, A.E. Orel, H.-D. Meyer, C.W. Mc Curdy, Phys. Rev. A **65**, 032716 (2002)
19. N. Chandra, A. Temkin, Phys. Rev. A **13**, 188 (1976)
20. E. Boronski, R.M. Nieminen, Phys. Rev. B **34**, 3820 (1986)
21. N.T. Padial, D.W. Norcross, Phys. Rev. A **29**, 1742 (1984)
22. W. Kohn, L.J. Sham, Phys. Rev. **140**, A1133 (1965)
23. F.A. Gianturco, A. Jain, Phys. Rep. **143**, 347 (1986)
24. M.J. Frish et al., *Gaussian 98, Revision A.7* (Pittsburg, PA: Gaussian Inc., 1998)
25. W.N. Sams, D.J. Kouri, J. Chem. Phys. **51**, 4809 (1969)
26. T.N. Rescigno, A.E. Orel, Phys. Rev. A **25**, 2402 (1982)
27. W.F. Murphy, J. Chem. Phys. **67**, 5877 (1977)
28. T. Shimanouchi, *Tables of molecular vibrational frequencies consolidated*, Vol. 1, National Standard Reference Data Series, National Bureau of Standards **39** (Washington, DC; US Goverment Printing Office, 1972), p. 10
29. I.G. John, G.B. Bacskay, N.S. Hush, Chem. Phys. **38**, 319 (1979)